Electronic supplementary information (ESI)

Copper-based ionic liquid-catalyzed click polymerization of diazides and diynes toward functional polytriazoles for sensing applications

Baixue Li, [†] Rong Hu, [†] Anjun Qin *,[†] and Ben Zhong Tang *,[†,‡]

[†] State Key Laboratory of Luminescent Materials and Devices, Guangdong Provincial Key Laboratory of Luminescence from Molecular Aggregates, Center for Aggregation-Induced Emission, South China University of Technology, Guangzhou 510640, China

[‡] Department of Chemistry, Hong Kong Branch of Chinese National Engineering Research Center for Tissue Restoration and Reconstruction, Institute for Advanced Study, and Department of Chemical and Biological Engineering, The Hong Kong University of Science & Technology, Clear Water Bay, Kowloon, Hong Kong, China

Table of Contents

Synthesis procedures of monomer **1a-1d**. S4

Synthesis procedures of monomer **2a-2c**. S4

Synthesis procedure of Cu-IL catalyst. S6

Cytotoxicity evaluation. S6

Binding behavior towards pathogens. S6

Cell imaging. S7

Table S1 Effect of solvent on the click polymerization. S7

Table S2 Effect of temperature on the click polymerization. S7

Table S3 Time course of the click polymerization. S8

Table S4 Effect of Cu-IL amount on the click polymerization. S8

Table S5 Effect of monomer concentration on the click polymerization. S8

Fig. S1 WAXD (A) and DSC curves (B) of P**1e2c**. S8

Fig. S2 TGA thermograms of polymers P**1a2a**-P**1e2c**. T_d presents the temperature of 5% weight loss. S9

Fig. S3 FT-IR spectra of **1b** (A), **2a** (B) and P**1b2a** (C). S9

Fig. S4 FT-IR spectra of **1c** (A), **2a** (B) and P**1c2a** (C). S10

Fig. S5 FT-IR spectra of **1d** (A), **2a** (B) and P**1d2a** (C). S10

Fig. S6 FT-IR spectra of **1b** (A), **2b** (B) and P**1b2b** (C). S11

Fig. S7 FT-IR spectra of **1e** (A), **2c** (B) and P**1e2c** (C). S11

Fig. S8 ^{1}H NMR spectra of **1b** (A), **2a** (B) and P**1b2a** (C) in $CDCl_3$. The solvent peaks are marked with asterisks. S12

Fig. S9 ^{1}H NMR spectra of **1c** (A), **2a** (B) and P**1c2a** (C) in $CDCl_3$. The solvent peaks are marked with asterisks. S13

Fig. S10 ^{1}H NMR spectra of **1d** (A), **2a** (B) and P**1d2a** (C) in $CDCl_3$. The solvent peaks are marked with asterisks. S14

Fig. S11 ^{1}H NMR spectra of **1b** (A), **2b** (B) and P**1b2b** (C) in $CDCl_3$. The solvent peaks are marked with asterisks. S15

Fig. S12 ^{1}H NMR spectra of **1e** (A), **2c** (B) and P**1e2c** (C) in DMSO-d_6. The solvent peaks are marked with asterisks. S16

Fig. S13 ^{13}C NMR spectra of **1b** (A), **2a** (B) and P**1b2a** (C) in $CDCl_3$. The solvent

peaks are marked with asterisks. S17

Fig. S14 ^{13}C NMR spectra of **1c** (A), **2a** (B) and P**1c2a** (C) in $CDCl_3$. The solvent peaks are marked with asterisks. S18

Fig. S15 ^{13}C NMR spectra of **1d** (A), **2a** (B) and P**1d2a** (C) in $CDCl_3$. The solvent peaks are marked with asterisks. S19

Fig. S16 ^{13}C NMR spectra of **1b** (A), **2b** (B) and P**1b2b** (C) in $CDCl_3$. The solvent peaks are marked with asterisks. S20

Fig. S17 ^{13}C NMR spectra of **1e** (A), **2c** (B) and P**1e2c** (C) in DMSO-d_6. The solvent peaks are marked with asterisks. S21

Fig. S18 (A) PL spectra of the P**1a2a** THF solutions containing different amounts of PA. Polymer concentration: 10 μM. λ_{ex}: 320 nm. (B) Stern-Volmer plots of $I_0/I - 1$ of P**1a2a** THF solution versus PA concentration, where I = peak intensity and I_0 = peak intensity at [PA] = 0 μg mL^{-1}. Inset: the chemical structure of PA. S21

Fig. S19 (A) PL decay curves of P**1e2c** aqueous solution at 450 nm in the presence of different amounts of PA. Polymer concentration: 10 μM; λ_{ex}: 340 nm. (B) Normalized absorption spectrum of PA and the PL spectrum of P**1e2c** aqueous solution. S22

Fig. S20 (A) PL decay curves of P**1e2c** at 450 nm aqueous solution with different amounts of Fe^{3+} ion. Polymer concentration: 10 μM; λ_{ex}: 340 nm. (B) Normalized absorption spectrum of Fe^{3+} ion and the PL spectrum of P**1e2c** aqueous solution. S22

Fig. S21 Cell viability of HeLa cells in the presence of P**1e2c** with different concentrations. S23

Fig. S22 FT-IR spectra of DEA (A) and Cu-IL (B). S23

Fig. S23 TGA thermograms of Cu-IL and DEA. T_d presents the temperature of 5% weight loss. S23

References S24

Synthesis procedures of monomer 1a-1d.

Synthesis of bis(4-azidophenyl)methane (**1a**)

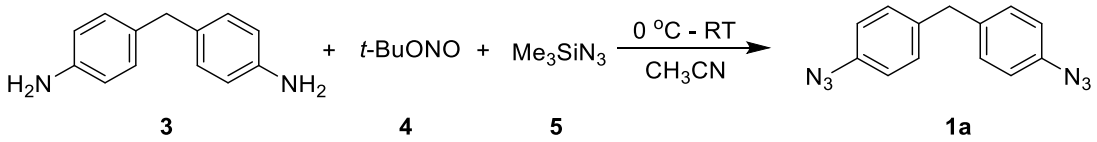

3 **4** **5** **1a**

This monomer was prepared according to previously published literature.[1]

Synthesis of 4,4'-oxybis(azidobenzene) (**1b**)

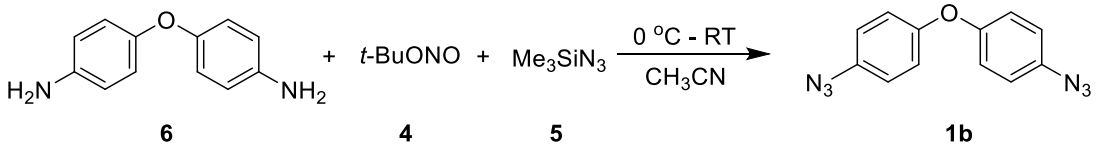

6 **4** **5** **1b**

This monomer was prepared according to previously published literature.[1]

FT-IR (KBr disk), ν (cm^{-1}): 2121 (−N_3 stretching), 1500, 1307, 1246, 1099, 839, 812, 534, 513. ^{1}H NMR (500 MHz, $CDCl_3$), δ (TMS, ppm): 6.99 (Ar-H). ^{13}C NMR (125 MHz, $CDCl_3$), δ (ppm): 154.50, 135.30, 120.55, 120.25.

Synthesis of 1,2-bis(4-azidophenyl)-1,2-diphenylethene (**1c**)

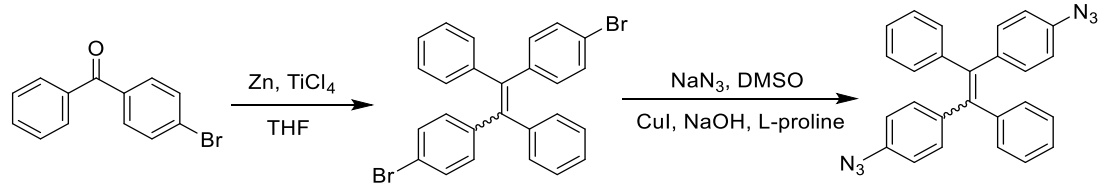

7 **8** **1c**

This monomer was prepared according to previously published literature.[2]

Synthesis of 1,2-bis(4-(azidomethyl)phenyl)-1,2-diphenylethene (**1d**)

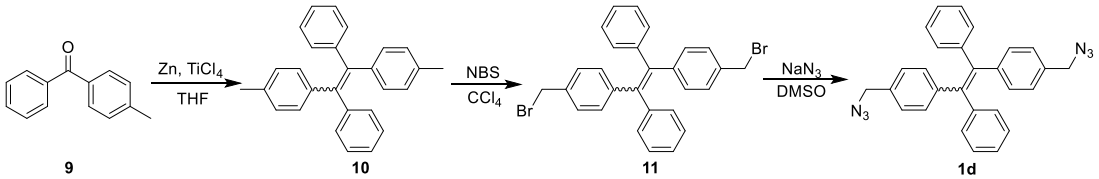

9 **10** **11** **1d**

This monomer was prepared according to previously published procedures.[3]

Synthesis procedures of monomer 2a-2c.

Synthesis of 2,7-diethynyl-9,9-dihexyl-9H-fluorene (**2a**)

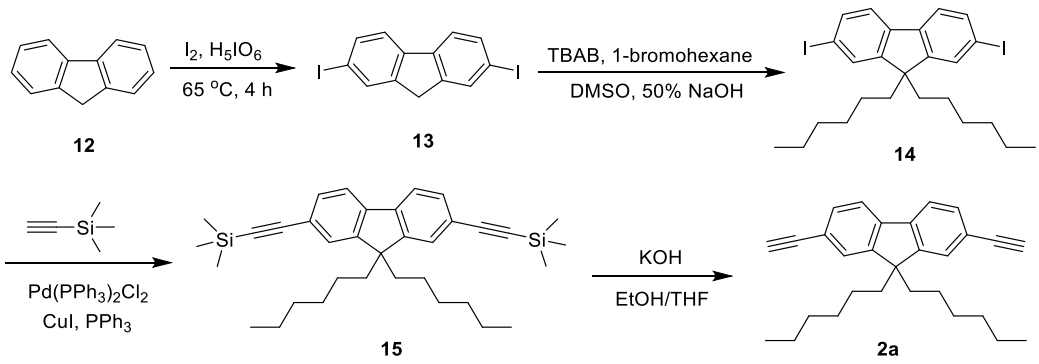

This monomer was prepared according to our previously published literatures.[4]

FT-IR (KBr disk), ν (cm^{-1}): 3303 (≡C–H stretching), 2931, 2855, 2107 (C≡C stretching), 1462, 888, 823, 647, 605. ^{1}H NMR (500 MHz, $CDCl_3$), δ (TMS, ppm): 7.64-7.46 (Ar-H), 3.15 (≡CH), 1.95, 1.10, 1.02, 0.77, 0.56. ^{13}C NMR (125 MHz, $CDCl_3$), δ (ppm): 151.11, 141.23, 131.50, 126.63, 121.12, 120.28, 84.86 (≡C–), 77.48 (≡CH), 55.30, 40.41, 31.66, 29.76, 23.76, 22.63, 14.16.

Synthesis of 2,7-diethynyl-9,9-dioctyl-9H-fluorene (**2b**)

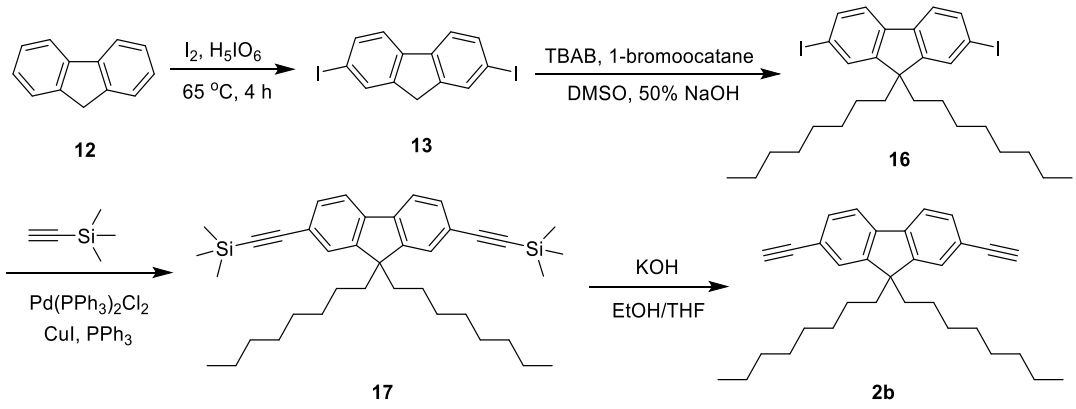

This monomer was prepared according to our previously published procedures.[4]

Synthesis of 2,5-diethynyl-1,4-phenylene tetraethyl bis(phosphate) (**2c**)

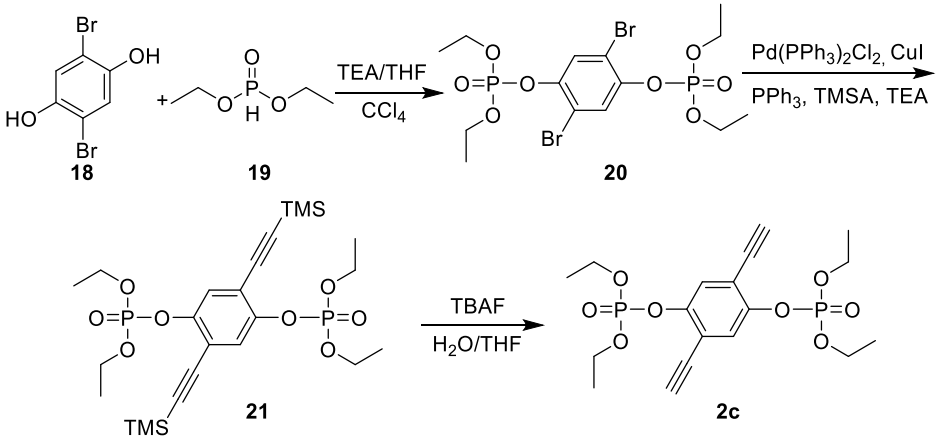

This monomer was prepared according to our previously published literatures.[4-6]

FT-IR (KBr disk), v (cm^{-1}): 3188 (≡C−H stretching), 2984, 2913, 2107 (C≡C stretching), 1493, 1392, 1282, 1268, 1189, 1164, 1051, 953, 892, 786, 746, 629, 521, 481, 463. ^{1}H NMR (500 MHz, DMSO-d_6), δ (TMS, ppm): 7.42 (Ar-H), 4.73 (≡CH), 4.21, 1.28. ^{13}C NMR (125 MHz, DMSO-d_6), δ (ppm): 147.51, 124.51, 116.26, 88.53 (≡C−), 77.10 (≡CH), 64.89, 15.86.

Synthesis procedure of Cu-IL catalyst.

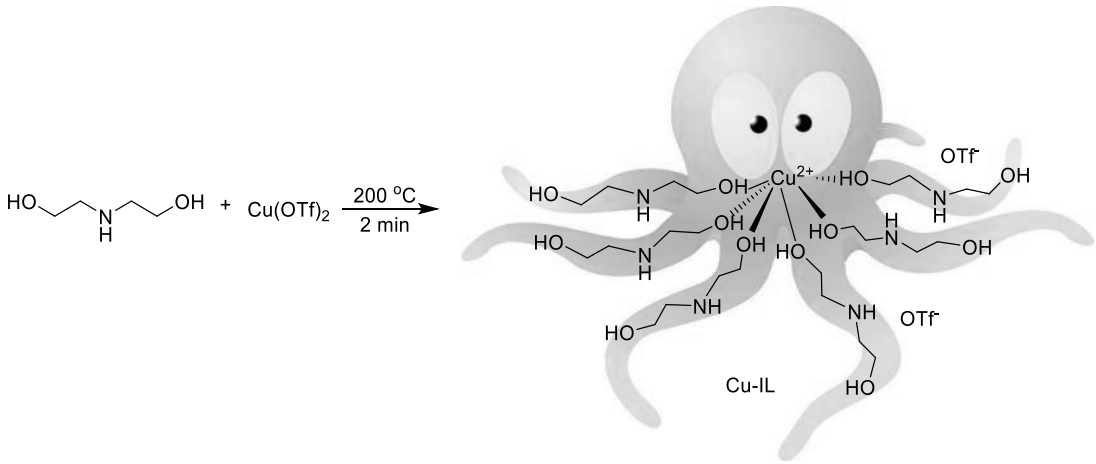

This Cu-IL was prepared according to previously published literature.[7,8]

Cytotoxicity evaluation.

HeLa cells were seeded in 96-well plate with 8×10^3 cells per well. After 24 h of culture, the medium was replaced by a series of different concentrations of P**1e2c** from 0 μM to 64 μM (100 μL $well^{-1}$). 24 h later, the medium was then exchanged by 100 μL of fresh medium containing 10 μL of MTT solution in each well and incubated at 37 °C for 4 h, and then 100 μL of DMSO was added to dissolve the purple crystals. The absorption was recorded by a microplate reader at 570 nm after shaking for 2 min. The cell viability ratio (VR) was evaluated according to the following equation:

$$\mathrm{VR} = \frac{A}{A_0} \times 100\%$$

Where A_0 is the absorbance of cells without any drugs, and A is the absorbance of cells incubated with P**1e2c**.

Binding behavior towards pathogens.

Preparation of bacterial solutions. A single colony of *S. aureus* on a solid Nutrient Broth (NB) agar plate was transferred to 10 mL of liquid Luria-Bertani (LB) culture medium

and grew at 37 ºC for 12 h. Bacteria were harvested by centrifuging (7100 rpm for 1 min) and washed by phosphate buffer saline (PBS, 10 mM, pH = 7.4) for three times. The supernatant was discarded and the remaining *S. aureus* was resuspended in PBS solution, and diluted to an optical density of 1.0 at 600 nm (OD_{600} = 1.0). As for *E. coli*, except that the culture medium was replaced by LB medium (with 10 μM Amp) other experimental conditions and operations were totally the same as that of *S. aureus*.

100 μL of bacterial solution (OD_{600} = 1.0) was added into PBS solution containing P**1e2c** (10 μM), followed by incubated at 37 ºC for 20 min. Individual aliquots of 3 μL of the pre-prepared mixed suspensions were added to clean glass slides followed by slightly covering coverslips for immobilization. The specimens were then examined by confocal laser scanning microscopy using a 405 nm laser.

Cell imaging.

HeLa cells were incubated with P**1e2c** (10 μM) in Dulbecco's modified Eagle medium (DMEM) containing 10% fetal bovine serum (FBS) for 1 h, 4 h and 12 h respectively, followed with the incubation of Lysotracker for 30 min. Then the species were observed on CLSM. 405 nm laser for P**1e2c**, and 488 nm for Lysotracker.

Table S1 Effect of solvent on the click polymerization[a]

Entry	Solvent	Yield (%)	M_w[b]	$Đ$[b]
1	DMF	94	77 900	2.71
2	Toluene	11	2600	1.05
3	1,4-Dioxane	14	2700	1.07
4	THF	Trace		

[a] Carried out at 50 ºC for 4 h under nitrogen, [Cu-IL]/[**1a**] = 0.1, [**1a**] = [**2a**] = 0.05 M. [b] Estimated by advanced polymer chromatography (APC) using THF as an eluent on the basis of a polystyrene (PS) calibration, M_w = weight-average molecular weight, polydispersity index ($Đ$) = M_w/M_n, M_n = number-average molecular weight.

Table S2 Effect of temperature on the click polymerization[a]

Entry	T (ºC)	Yield (%)	M_w[b]	$Đ$[b]
1	30	63	6800	1.42
2	40	90	45 500	2.49
3[c]	50	94	77 900	2.71

[a] Carried out in DMF for 4 h under nitrogen, [Cu-IL]/[**1a**] = 0.1, [**1a**] = [**2a**] = 0.05 M. [b] Estimated by APC using THF as an eluent on the basis of a PS calibration, M_w = weight-average molecular weight, $Đ$ = M_w/M_n, M_n = number-average molecular weight. [c] Data taken from Table S1, entry 1.

Table S3 Time course of the click polymerization[a]

Entry	*t* (h)	Yield (%)	M_w[b]	$Đ$[b]
1	1	57	6300	1.33
2	2	90	59 900	2.47
3	3	88	76 900	2.53
4[c]	4	94	77 900	2.71

[a] Carried out in DMF at 50 °C under nitrogen, [Cu-IL]/[**1a**] = 0.1, [**1a**] = [**2a**] = 0.05 M. [b] Estimated by APC using THF as an eluent on the basis of a PS calibration, M_w = weight-average molecular weight, $Đ = M_w/M_n$, M_n = number-average molecular weight. [c] Data taken from Table S2, entry 3.

Table S4 Effect of Cu-IL amount on the click polymerization[a]

Entry	Cu-IL (mol%)	Yield (%)	M_w[b]	$Đ$[b]
1[c]	10.0	90	59 900	2.47
2	5.0	92	77 800	2.67
3	2.5	22	4400	1.22

[a] Carried out in DMF at 50 °C for 2 h under nitrogen, [**1a**] = [**2a**] = 0.05 M. [b] Estimated by APC using THF as an eluent on the basis of a PS calibration, M_w = weight-average molecular weight, $Đ = M_w/M_n$, M_n = number-average molecular weight. [c] Data taken from Table S3, entry 2.

Table S5 Effect of monomer concentration on the click polymerization[a]

Entry	[M] (mol/L)	Yield (%)	M_w[b]	$Đ$[b]
1[c]	0.050	92	77 800	2.67
2	0.040	94	39 700	2.76
3	0.033	84	14 700	1.98
4	0.025	28	4700	1.22

[a] Carried out in DMF at 50 °C for 2 h under nitrogen, [Cu-IL]/[**1a**] = 0.05, [**1a**] = [**2a**]. [b] Estimated by APC using THF as an eluent on the basis of a PS calibration, M_w = weight-average molecular weight, $Đ = M_w/M_n$, M_n = number-average molecular weight. [c] Data taken from Table S4, entry 2.

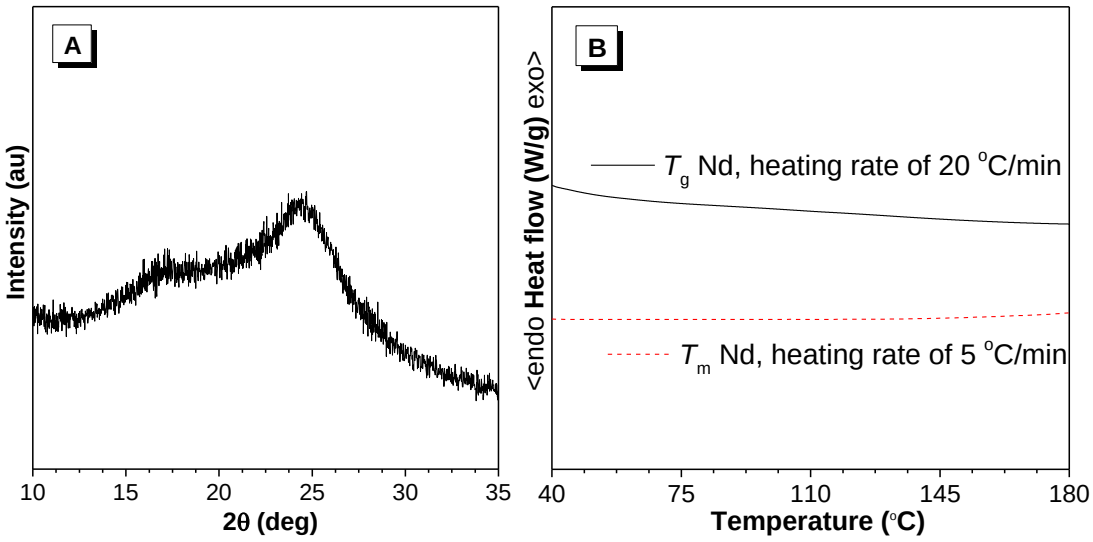

Fig. S1 WAXD (A) and DSC curves (B) of P**1e2c**.

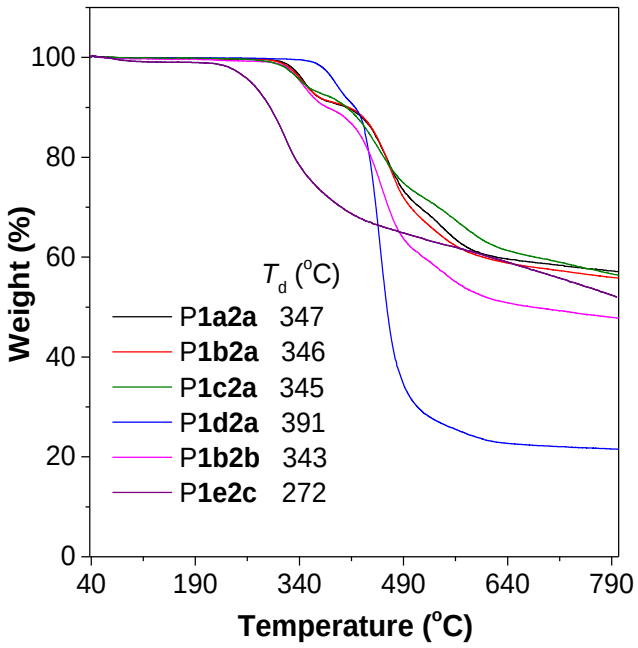

Fig. S2 TGA thermograms of polymers P**1a2a**-P**1e2c**. T_d presents the temperature of 5% weight loss.

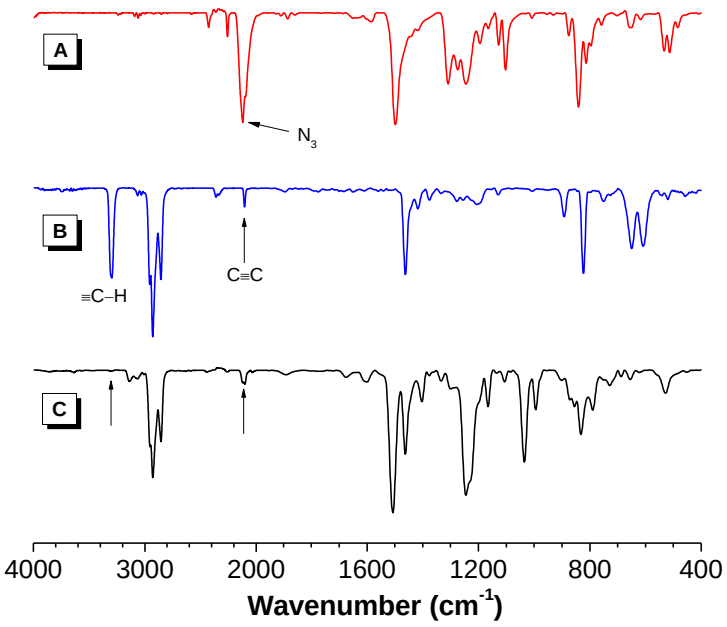

Fig. S3 FT-IR spectra of **1b** (A), **2a** (B) and P**1b2a** (C).

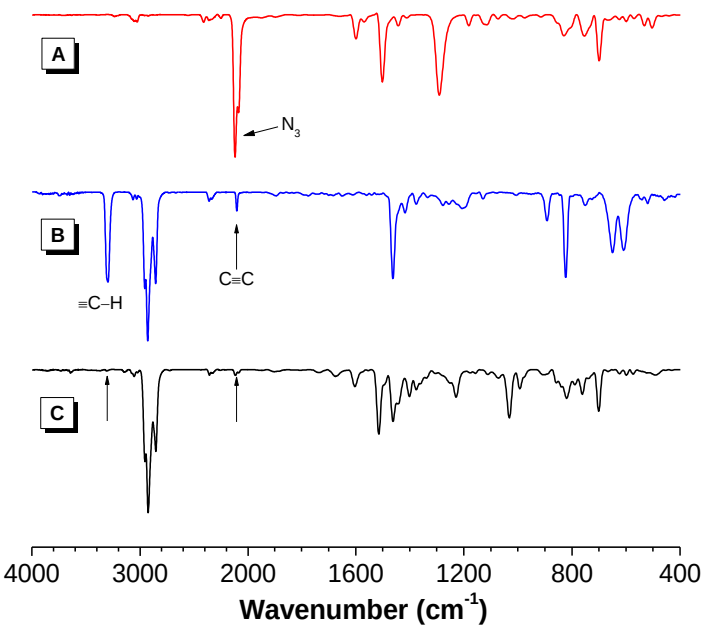

Fig. S4 FT-IR spectra of **1c** (A), **2a** (B) and P**1c2a** (C).

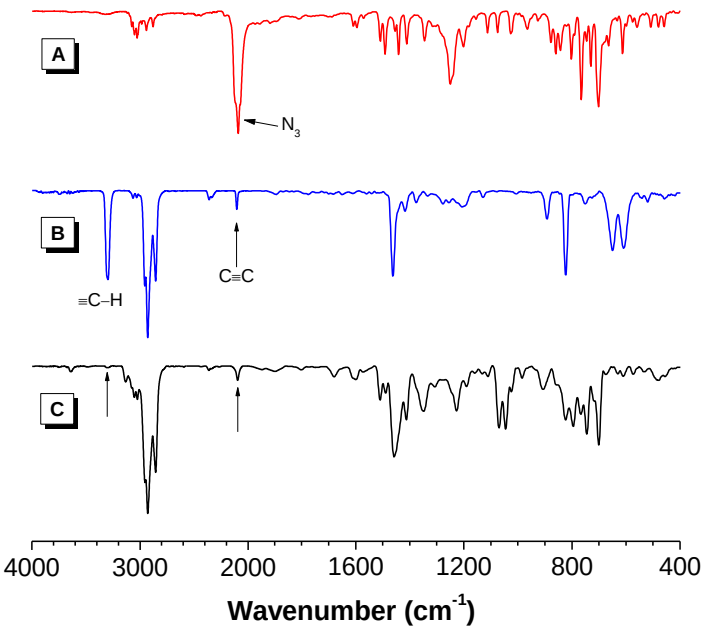

Fig. S5 FT-IR spectra of **1d** (A), **2a** (B) and P**1d2a** (C).

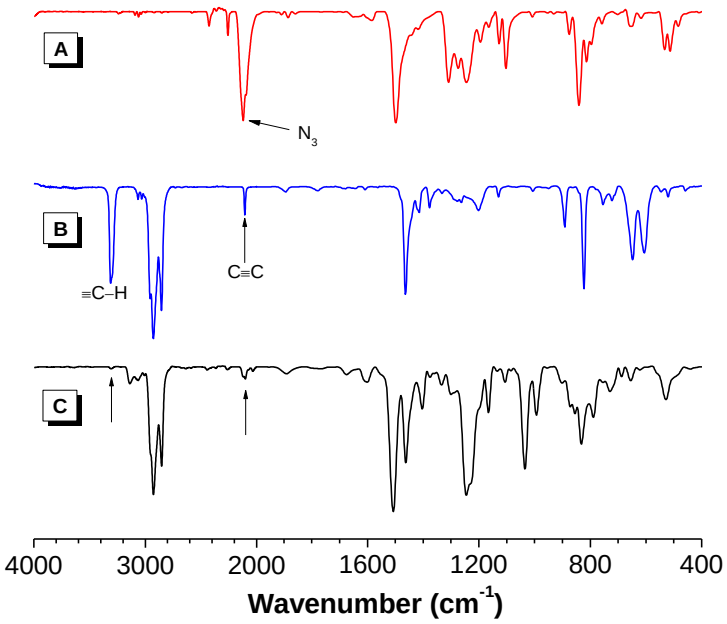

Fig. S6 FT-IR spectra of **1b** (A), **2b** (B) and P**1b2b** (C).

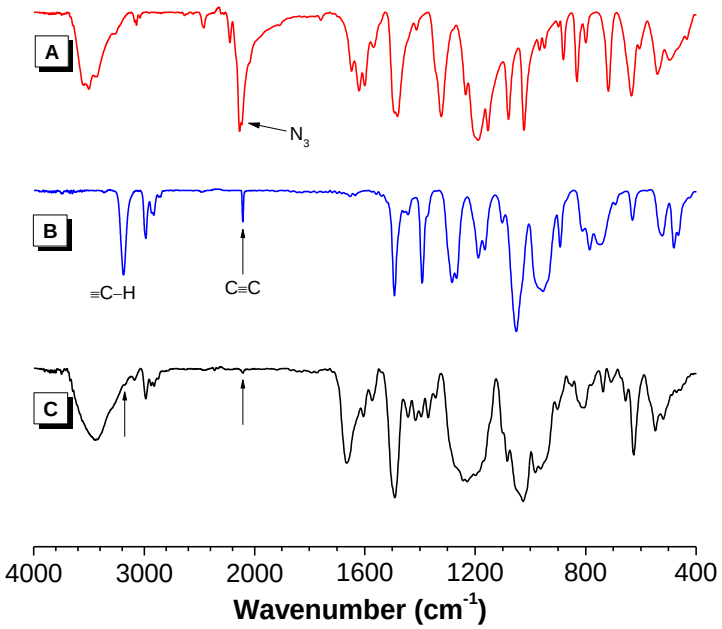

Fig. S7 FT-IR spectra of **1e** (A), **2c** (B) and P**1e2c** (C).

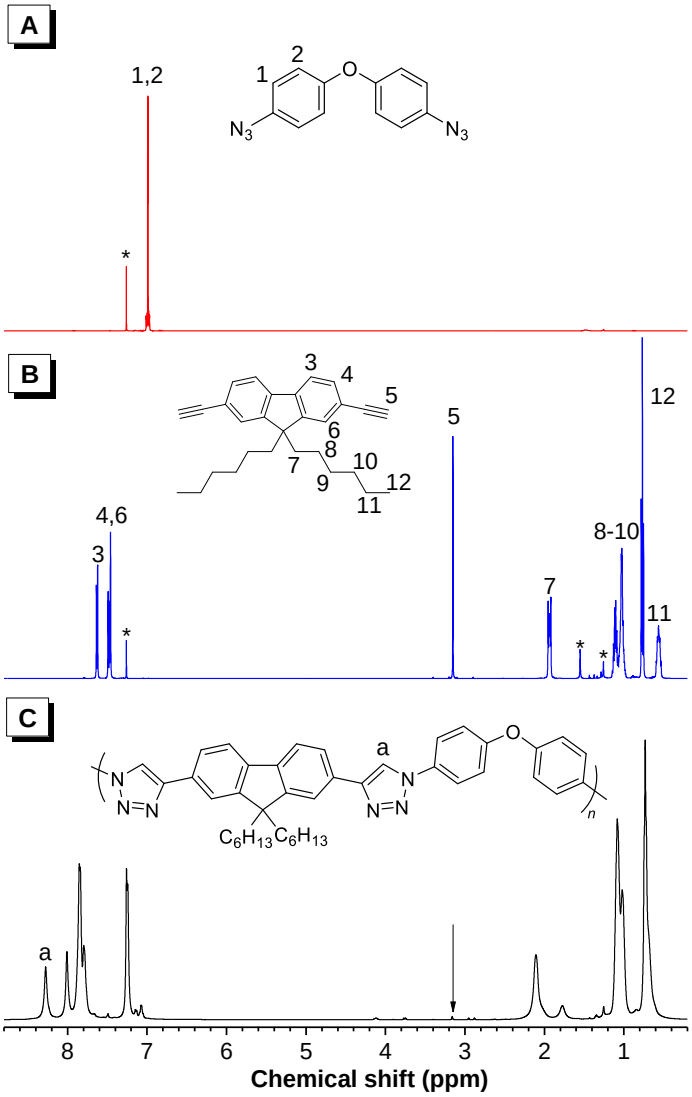

Fig. S8 ^{1}H NMR spectra of **1b** (A), **2a** (B) and P**1b2a** (C) in $CDCl_3$. The solvent peaks are marked with asterisks.

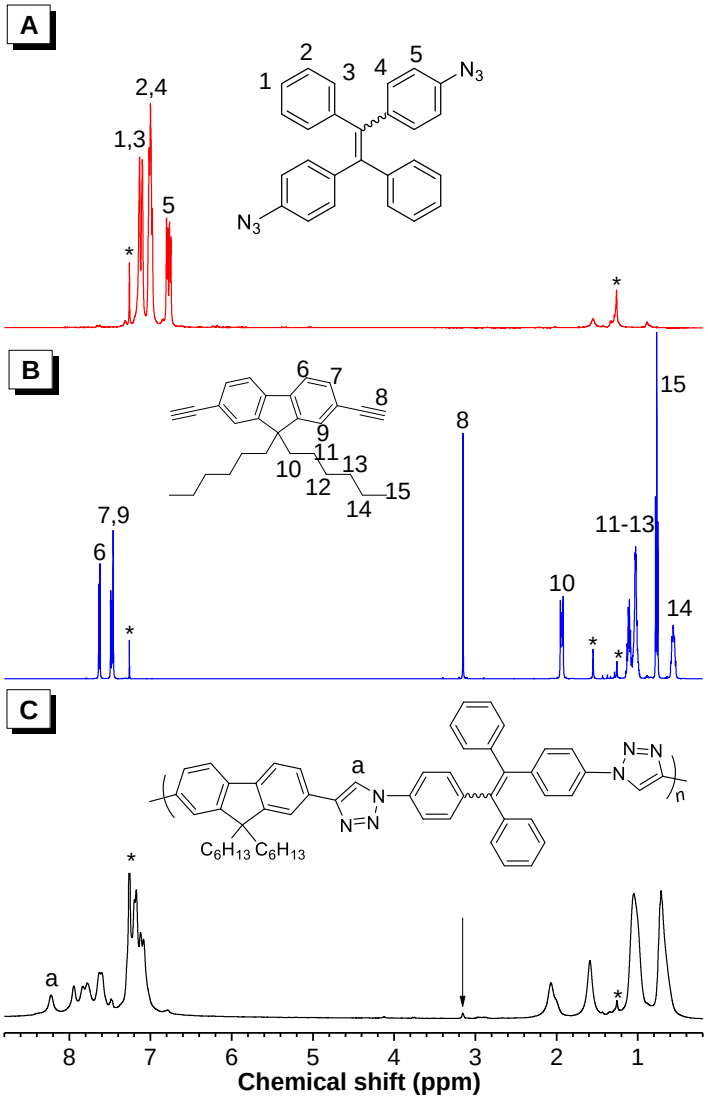

Fig. S9 ^{1}H NMR spectra of **1c** (A), **2a** (B) and P**1c2a** (C) in $CDCl_3$. The solvent peaks are marked with asterisks.

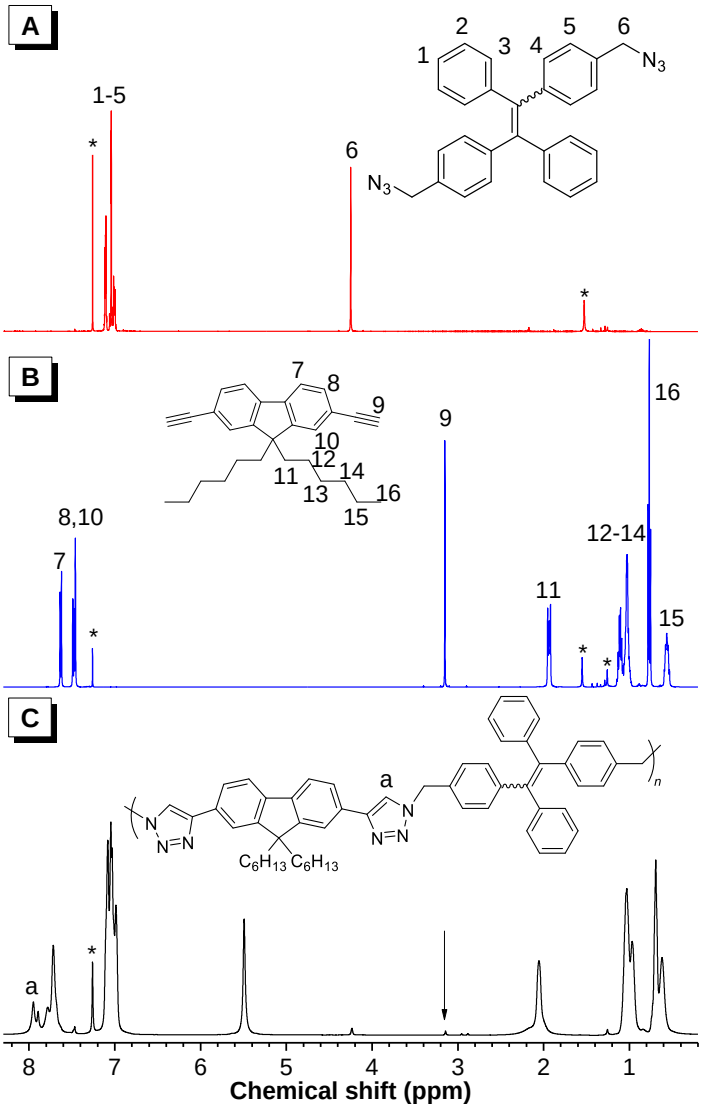

Fig. S10 ^{1}H NMR spectra of **1d** (A), **2a** (B) and P**1d2a** (C) in $CDCl_3$. The solvent peaks are marked with asterisks.

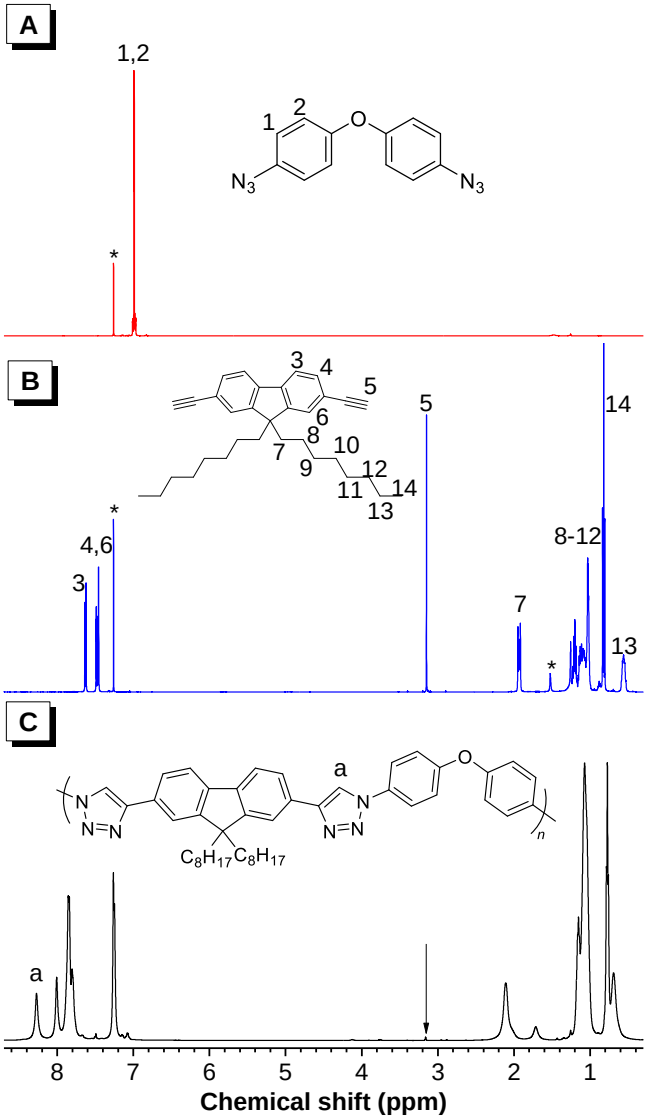

Fig. S11 ^{1}H NMR spectra of **1b** (A), **2b** (B) and P**1b2b** (C) in $CDCl_3$. The solvent peaks are marked with asterisks.

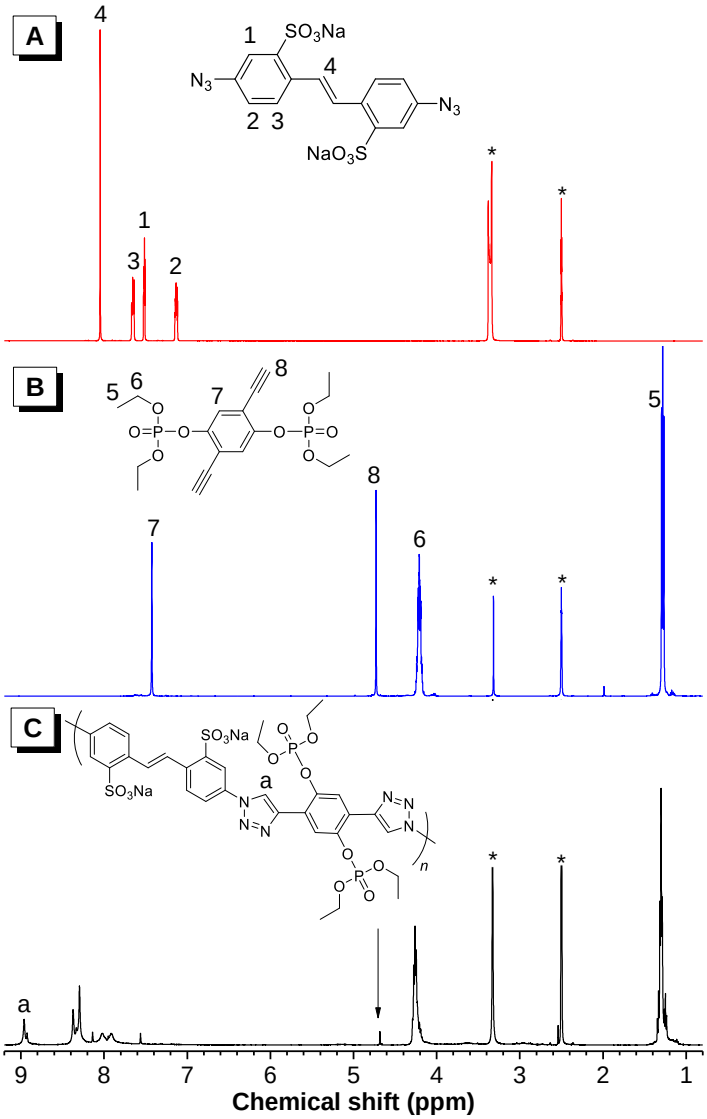

Fig. S12 ^{1}H NMR spectra of **1e** (A), **2c** (B) and P**1e2c** (C) in DMSO-d_6. The solvent peaks are marked with asterisks.

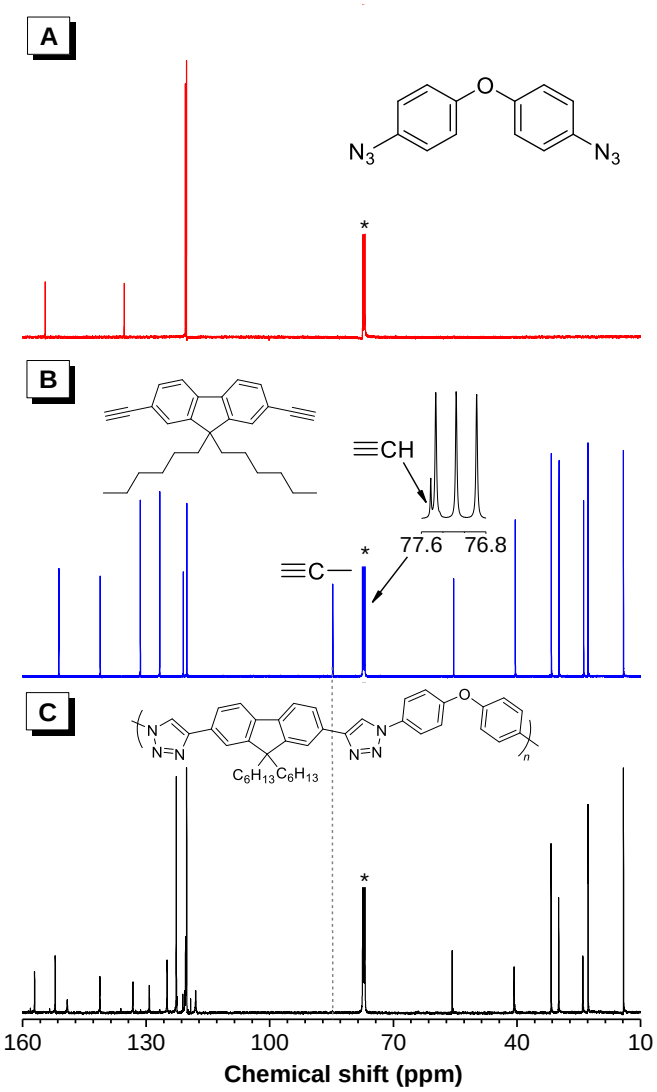

Fig. S13 ^{13}C NMR spectra of **1b** (A), **2a** (B) and P**1b2a** (C) in $CDCl_3$. The solvent peaks are marked with asterisks.

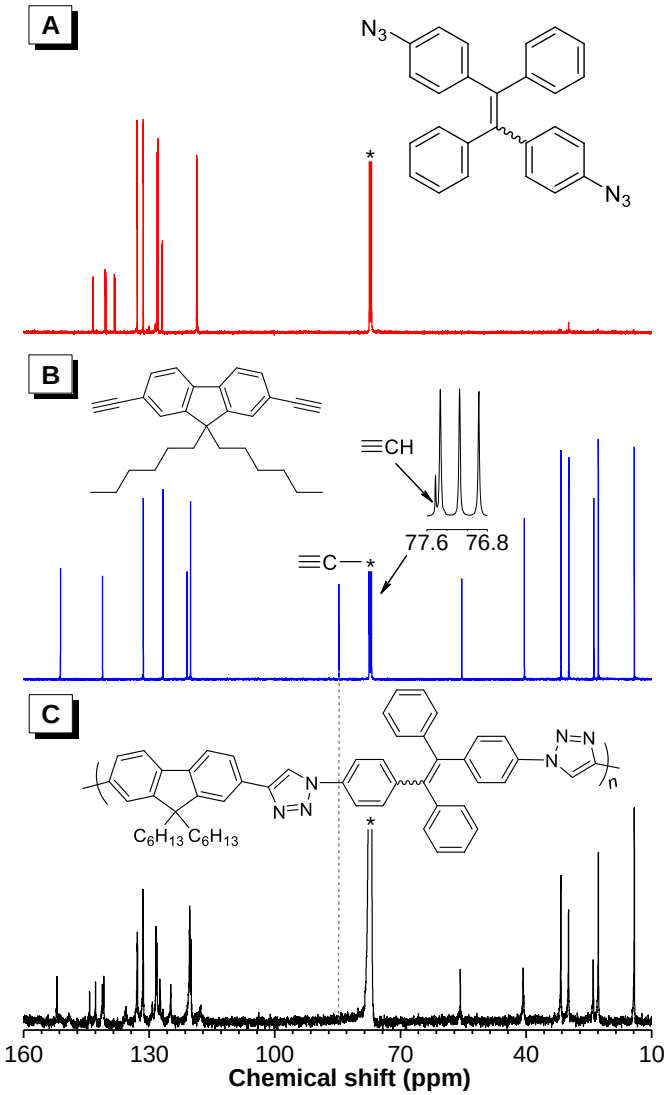

Fig. S14 ^{13}C NMR spectra of **1c** (A), **2a** (B) and P**1c2a** (C) in $CDCl_3$. The solvent peaks are marked with asterisks.

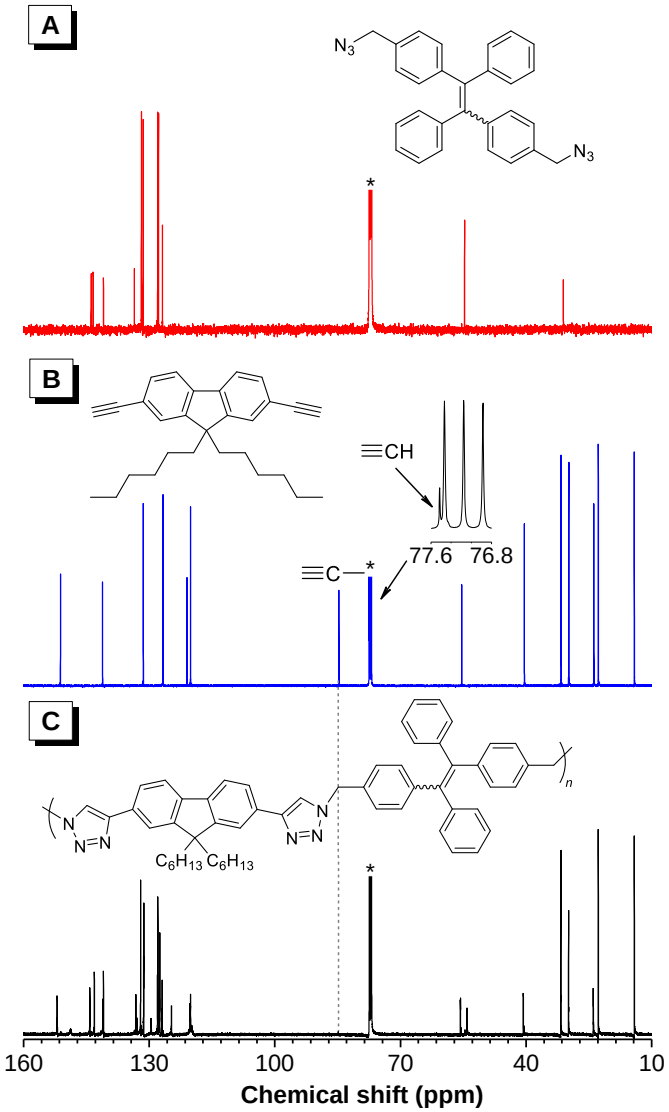

Fig. S15 ^{13}C NMR spectra of **1d** (A), **2a** (B) and P**1d2a** (C) in $CDCl_3$. The solvent peaks are marked with asterisks.

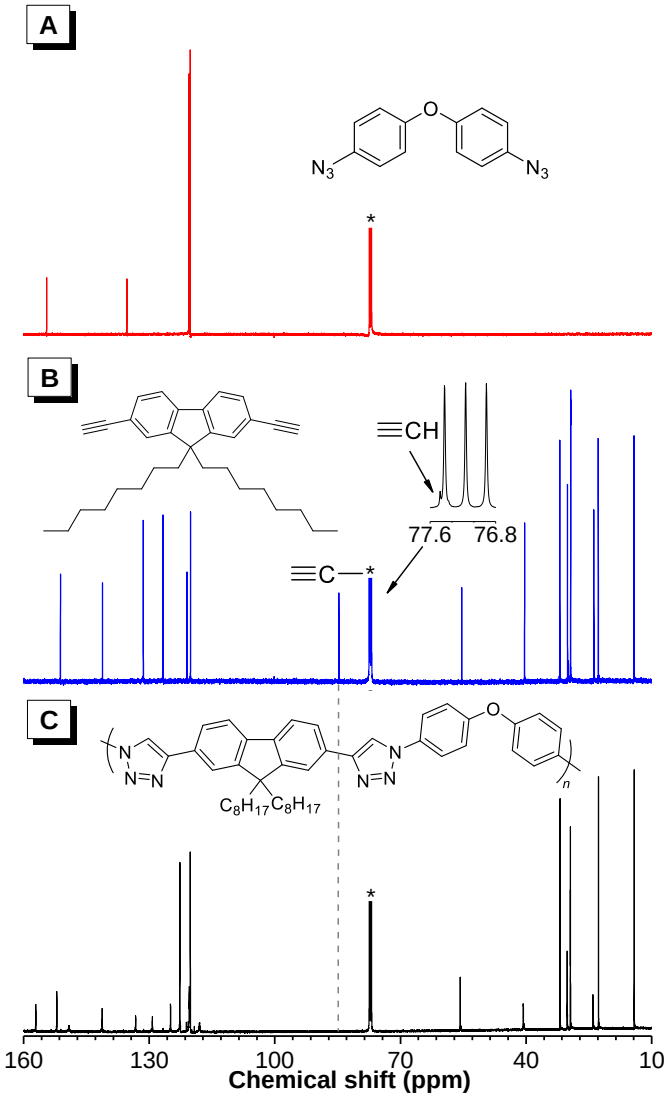

Fig. S16 ^{13}C NMR spectra of **1b** (A), **2b** (B) and P**1b2b** (C) in $CDCl_3$. The solvent peaks are marked with asterisks.

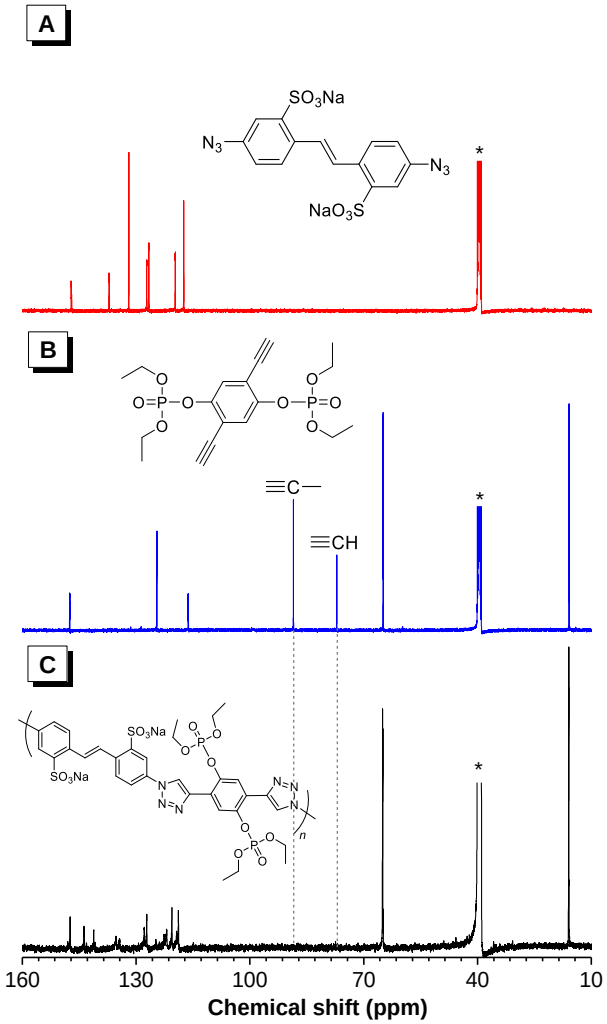

Fig. S17 ^{13}C NMR spectra of **1e** (A), **2c** (B) and P**1e2c** (C) in DMSO-d_6. The solvent peaks are marked with asterisks.

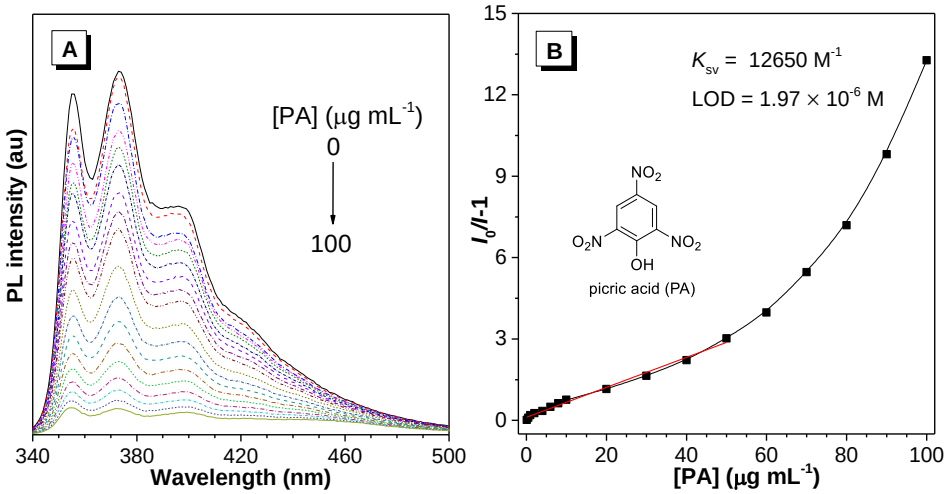

Fig. S18 (A) PL spectra of the P**1a2a** THF solutions containing different amounts of PA. Polymer concentration: 10 μM. λ_{ex}: 320 nm. (B) Stern-Volmer plots of I_0/I −1 of P**1a2a** THF solution versus PA concentration, where I = peak intensity and I_0 = peak intensity at [PA] = 0 μg mL^{-1}. Inset: the chemical structure of PA.

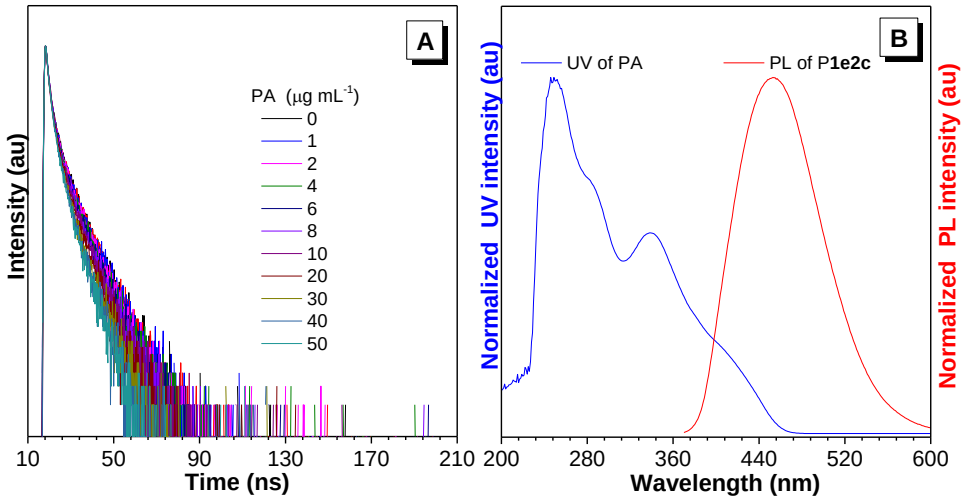

Fig. S19 (A) PL decay curves of P**1e2c** aqueous solution at 450 nm in the presence of different amounts of PA. Polymer concentration: 10 μM; λ_{ex}: 340 nm. (B) Normalized absorption spectrum of PA and the PL spectrum of P**1e2c** aqueous solution.

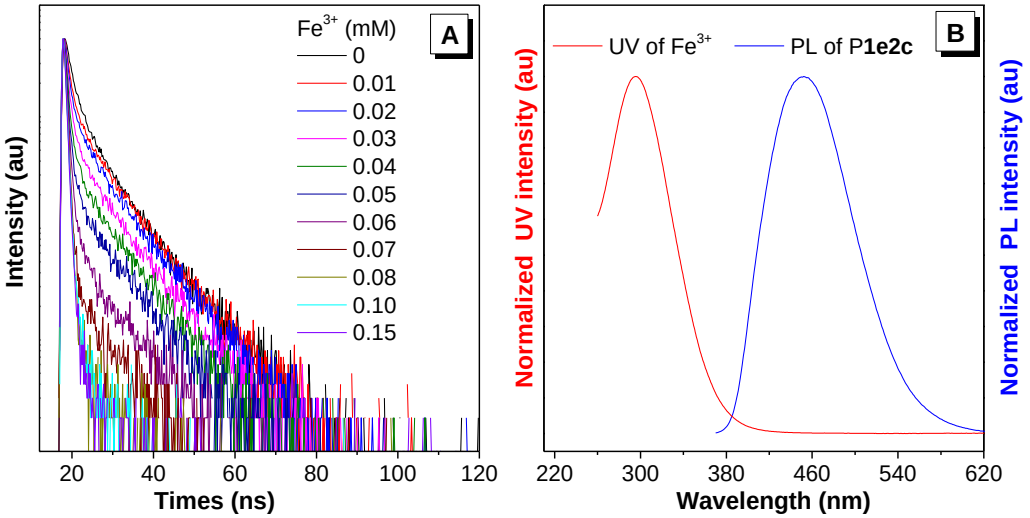

Fig. S20 (A) PL decay curves of P**1e2c** at 450 nm aqueous solution with different amounts of Fe^{3+} ion. Polymer concentration: 10 μM; λ_{ex}: 340 nm. (B) Normalized absorption spectrum of Fe^{3+} ion and the PL spectrum of P**1e2c** aqueous solution.

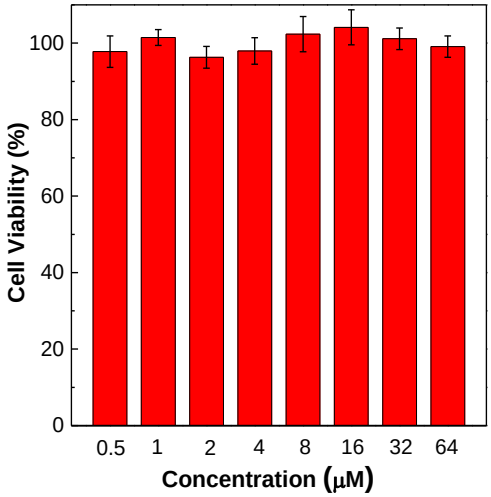

Fig. S21 Cell viability of HeLa cells in the presence of P**1e2c** with different concentrations.

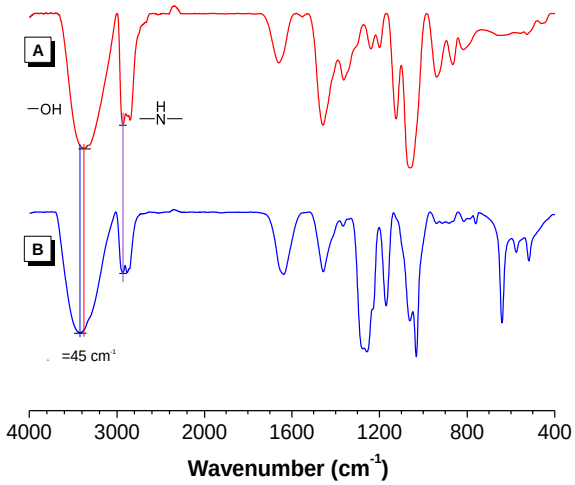

Fig. S22 FT-IR spectra of DEA (A) and Cu-IL (B).

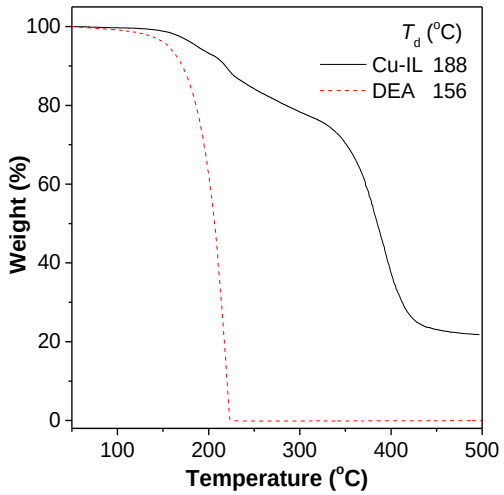

Fig. S23 TGA thermograms of Cu-IL and DEA. T_d presents the temperature of 5% weight loss.

References

(1) Y. Zhao and T. M. Swager, *Eur. J. Org. Chem*., 2015, **2015**, 4593−4597.

(2) J. Wang, J. Mei, E. Zhao, Z. Song, A. Qin, J. Z. Sun and B. Z. Tang, *Macromolecules*, 2012, **45**, 7692−7703.

(3) A. Qin, L. Tang, J. W. Y. Lam, C. K. W. Jim, Y. Yu, H. Zhao, J. Z. Sun and B. Z. Tang, *Adv. Funct. Mater*., 2009, **19**, 1891−1900.

(4) E. Zhao, H. Li, J. Ling, H. Wu, J. Wang, S. Zhang, J. W. Y. Lam, J. Z. Sun, A. Qin and B. Z. Tang, *Polym. Chem*., 2014, **5**, 2301−2308.

(5) S. S. L. Corre, M. Berchel, H. C. Gourvès, J. P. Haelters and P. A. Jaffrès, *Beilstein J. Org. Chem*., 2014, **10**, 1166−1196.

(6) R. Hu, R. Ye, J. W. Y. Lam, M. Li, C. W. T. Leung and B. Z. Tang, *Chem.—Asian J*., 2013, **8**, 2436−2445.

(7) B. Mohan, H. Kang and K. H. Park, *Inorg. Chem. Commun*., 2013, **35**, 239−241.

(8) H. D. Pratt III, A. J. Rose, C. L. Staiger, D. Ingersoll and T. M. Anderson, *Dalton Trans*., 2011, **40**, 11396−11401.